

Preconditioning for finite element methods with strain smoothing^{*}

Chaemin Lee^{a,*}, Jongho Park^b

^a*Department of Mechanical Engineering, KAIST, Daejeon 34141, Korea*

^b*Natural Science Research Institute, KAIST, Daejeon 34141, Korea*

Abstract

Strain smoothing methods such as the smoothed finite element methods (S-FEMs) and the strain-smoothed element (SSE) method have successfully improved the performance of finite elements, and there have been numerous applications of them in finite element analysis. For the sake of efficient applications to large-scale problems, it is important to develop a mathematically and numerically well-elaborated iterative solver for the strain smoothing methods. In this paper, inspired by the spectral properties of the strain smoothing methods, we propose efficient ways of preconditioning for the methods. First, we analyze the spectrums of the stiffness matrices of the edge-based S-FEM and the SSE method. Then, we propose an improved two-level additive Schwarz preconditioner for the strain smoothing methods by modifying local solvers appropriately. For the sake of convenience of implementation, an alternative form of the preconditioner is also proposed by defining the coarse-scale operation in terms of the standard FEM. We verify our theoretical results through numerical experiments.

Keywords: Finite element method, Smoothed finite element method, Strain-smoothed element method, Preconditioning, Additive Schwarz method
2020 MSC: 65F08, 65N30, 74S05, 65N55

1. Introduction

There have been various attempts to improve the performance of finite elements, among which strain smoothing methods can improve the performance of finite elements without introducing additional degrees of freedom. The concept of strain smoothing methods was first proposed in a pioneering work of Chen et al. [1] for the Galerkin mesh-free method. Then, Liu et al. [2] applied the strain smoothing technique to the finite element method (FEM), and developed a series of smoothed FEMs (S-FEMs). The S-FEMs are classified according to the way of defining smoothing domains; the edge-based S-FEM (ES-FEM) and node-based S-FEM (NS-FEM) are well-known and broadly used [3, 4, 5, 6, 7]. The ES-FEM generally exhibits the most superior convergence properties among the S-FEMs [4], and the NS-FEM is effective in relieving volumetric locking [3]. Several studies were conducted to establish the theoretical properties of the S-FEMs [5, 8, 9]. Recently, the strain-smoothed element (SSE) method has been developed [10, 11, 12]. Whereas the S-FEMs construct strain fields for specifically defined smoothing domains, the SSE method constructs strain fields for elements. The SSE method shows high predictive capability by fully using the strains of all neighboring elements for strain smoothing. A theoretical foundation for the convergence properties of the SSE method has been established in [13].

As we saw above, strain smoothing has been an interesting topic of the development and improvement of finite elements over the past decades. Even though there has been a vast literature on the development of new strain smoothing methods and their applications to various engineering problems (see [14] for a recent survey), to the best of

^{*}Chaemin Lee's work was supported by Basic Science Research Program through the National Research Foundation of Korea (NRF) funded by the Ministry of Education (No. 2021R1A6A3A01086822). Jongho Park's work was supported by the National Research Foundation of Korea (NRF) grant funded by the Korea government (MSIT) (No. 2021R1C1C2095193).

^{*}Corresponding author

Email addresses: ghi9000@kaist.ac.kr (Chaemin Lee), jongho.park@kaist.ac.kr (Jongho Park)

URL: <https://sites.google.com/view/jonghopark> (Jongho Park)

our knowledge, there have been no existing works about efficient numerical solvers for the strain smoothing methods. However, developing robust and efficient numerical solvers is an important issue for the sake of successful applications of the methods to large-scale engineering problems [15]. In particular, iterative solvers are suitable to be applied to large-scale sparse linear problems [16]. Since the performance of iterative solvers mainly relies on the condition number of a target linear system, an effective way to improve iterative solvers is to design good preconditioners. In this perspective, there have been plenty of notable works on preconditioning of large-scale linear problems arising in structural mechanics; see, e.g., [17, 18, 19, 20].

In this paper, we deal with efficient iterative solvers for the strain smoothing methods. The main observation is that the stiffness matrices of the ES-FEM and SSE method are spectrally equivalent to that of the standard FEM. This observation guarantees that both the ES-FEM and SSE method can adopt any preconditioner designed for the standard FEM and enjoy the advantages of the preconditioner such as good conditioning or numerical scalability. As a concrete example, we consider overlapping Schwarz preconditioner, which is one of the most broadly used parallel preconditioners for finite element problems [21, 22, 23, 24]. We prove that the standard two-level additive Schwarz preconditioner [21] designed for the standard FEM can be applied to the ES-FEM and SSE method, satisfying the condition number bound $C(1 + H/\delta)$, where C is a positive constant independent of the mesh and subdomain sizes, H is the subdomain size, and δ is the overlapping width for the overlapping domain decomposition associated with the additive Schwarz preconditioner. In addition, we propose novel improved two-level additive Schwarz preconditioners for the ES-FEM and SSE method with better condition number estimates than the standard two-level additive Schwarz preconditioner. With some simple modifications on the local problems of the standard Schwarz preconditioner, we obtain the proposed preconditioners that show the improved performance in both theoretical and numerical senses. The improvement strategy can be applied to not only additive Schwarz preconditioners but also a broad range of subspace correction preconditioners [25, 26] such as multigrid and domain decomposition preconditioners. Noting that many existing iterative solvers for linear systems fit into the framework of subspace correction [25], the improvement strategy introduced in this paper opens up new possibilities for designing efficient iterative solvers for various contemporary FEMs. Numerical results verify the theories presented in this paper and highlight the superiority of the proposed improved preconditioners.

This paper includes another interesting remark on the NS-FEM; even though the NS- and ES-FEM are considered as members of the common class of S-FEMs, their spectral properties may be quite different. In this paper, we claim that the stiffness matrix of the NS-FEM may not be spectrally equivalent to that of the standard FEM. More precisely, we present an example that the condition number $\kappa(K^{-1}\tilde{K}_{\text{NS}})$ increases as the mesh size h decreases, where K and \tilde{K}_{NS} are the stiffness matrices of the standard FEM and NS-FEM, respectively. This suggests the necessity to develop a mathematical theory for the NS-FEM separated from the ES-FEM, while most of the existing theories [5, 9, 14] are based on a unified S-FEM framework.

The remainder of this paper is organized as follows. In Section 2, we briefly summarize key features of the ES-FEM and SSE method. Section 3 deals with the spectral properties of the ES-FEM and SSE method; more precisely, we show that the stiffness matrices of these methods are spectrally equivalent to that of the standard FEM. Utilizing the spectral equivalence, in Section 4, we present efficient two-level additive Schwarz preconditioners for the ES-FEM and SSE method and analyze their convergence properties. Section 5 presents numerical results that support our theoretical findings. In Section 6, we give some remarks on the spectral property of the NS-FEM. We conclude our paper in Section 7.

2. Finite element methods with strain smoothing

We provide brief descriptions of the S-FEM and SSE method for a model Poisson problem

$$\begin{aligned} -\Delta u &= f && \text{in } \Omega, \\ u &= 0 && \text{on } \partial\Omega, \end{aligned}$$

where $\Omega \subset \mathbb{R}^2$ is a bounded polygonal domain. For simplicity, we consider the case of three-node triangular elements throughout this paper; see [27] and [12] for formulations of polygonal finite elements adopting the S-FEM and SSE method, respectively. Let \mathcal{T}_h be a quasi-uniform triangulation of Ω with a maximum element diameter $h > 0$. We

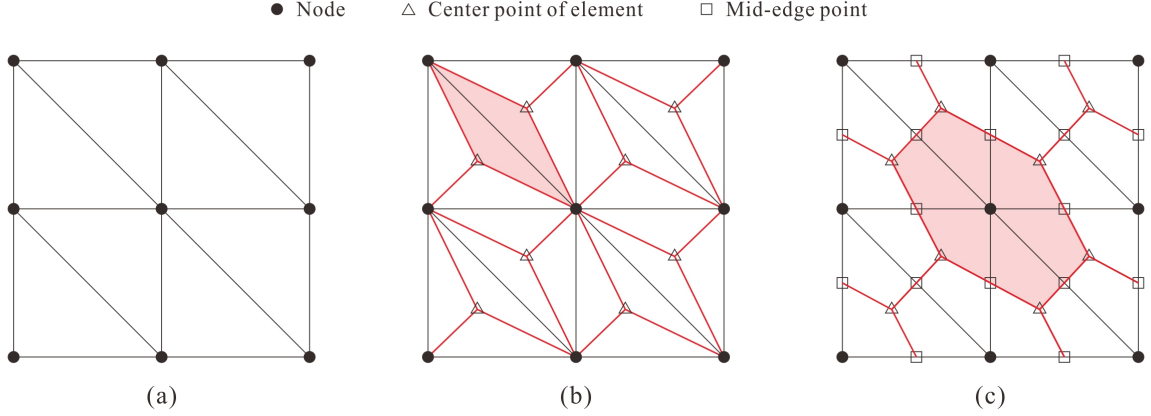


Figure 1: Discretizations based on (a) finite elements, (b) edge-based smoothing domains, and (c) node-based smoothing domains.

define V_h as the conforming piecewise linear finite element space on \mathcal{T}_h , i.e.,

$$V_h = \left\{ v \in H_0^1(\Omega) : v|_e \in \mathcal{P}_1(e) \quad \forall e \in \mathcal{T}_h \right\},$$

where $H_0^1(\Omega)$ is the usual Sobolev space consisting of all functions $u \in L^2(\Omega)$ such that $\nabla u \in (L^2(\Omega))^2$ and $u|_{\partial\Omega} = 0$. In what follows, with a slight abuse of notation, we do not distinguish between finite element functions and the corresponding vectors of degrees of freedom.

2.1. Standard finite element method

The geometry of a 3-node triangular element $e \in \mathcal{T}_h$ is interpolated by

$$(x, y) = \sum_{i=1}^3 h_i(r, s)(x_i, y_i) \in e,$$

where (x_i, y_i) , $1 \leq i \leq 3$, is the position vector of the i th node of e in the global Cartesian coordinate system, and $h_i(r, s)$ is the two-dimensional interpolation function of the standard isoparametric procedure corresponding to the i th node, i.e., $h_1(r, s) = 1 - r - s$, $h_2(r, s) = r$, and $h_3(r, s) = s$. The corresponding interpolation of the function u within the element e is given by

$$u(x, y) = \sum_{i=1}^3 h_i(r, s)u_i,$$

where $u_i = u(x_i, y_i)$. Note that u is continuous and piecewise linear on \mathcal{T}_h , i.e., $u \in V_h$.

The local gradient $\epsilon^{(e)}$ within the element e is obtained through the standard isoparametric finite element procedure as follows:

$$\epsilon^{(e)} = B^{(e)} u^{(e)} \quad \text{with} \quad B^{(e)} = \begin{bmatrix} \frac{\partial h_1}{\partial x} & \frac{\partial h_2}{\partial x} & \frac{\partial h_3}{\partial x} \\ \frac{\partial h_1}{\partial y} & \frac{\partial h_2}{\partial y} & \frac{\partial h_3}{\partial y} \end{bmatrix}, \quad u^{(e)} = [u_1 \quad u_2 \quad u_3]^T. \quad (2.1)$$

Now, the stiffness matrix K corresponding to the standard FEM is given by

$$u^T K v = \int_{\Omega} \nabla u \cdot \nabla v \, d\Omega = \sum_{e \in \mathcal{T}_h} |e| (B^{(e)} u^{(e)})^T (B^{(e)} v^{(e)}), \quad u, v \in V_h. \quad (2.2)$$

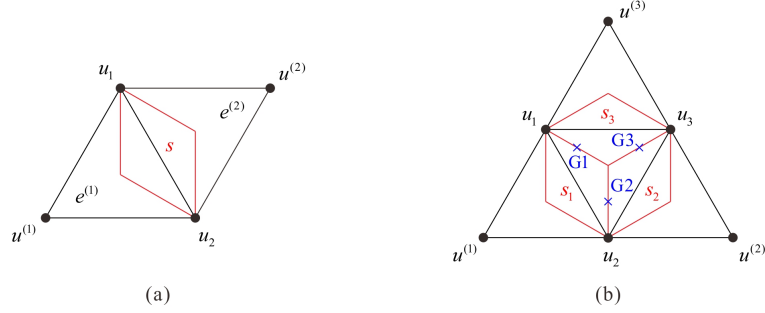


Figure 2: Degrees of freedom of $u \in V_h$ corresponding to the vectors (a) $\bar{u}^{(s)}$ in (2.4) and (b) $\bar{u}^{(e)}$ in (2.8).

2.2. Edge-based smoothed finite element method

Whereas the standard FEM discretizes a region into finite elements (see Fig. 1(a)), S-FEM performs discretization based on newly defined smoothing domains. The most well-known S-FEMs are the ES-FEM and NS-FEM, which form the smoothing domains based on edges and nodes of \mathcal{T}_h , respectively. Here, we briefly introduce the ES-FEM; see Section 6 for a description of the NS-FEM.

In the ES-FEM, each element in \mathcal{T}_h is divided into three triangular subdomains using its nodes and the center point ($r = s = 1/3$). Then, the edge-based smoothing domains are defined as assemblages of two neighboring subdomains belonging to different elements; see Fig. 1(b). In the following, let $\mathcal{S}_{h,ES}$ denote the collection of all smoothing domains constructed from \mathcal{T}_h for the ES-FEM. A local smoothed gradient $\bar{\epsilon}^{(s)}$ for a smoothing domain $s \in \mathcal{S}_{h,ES}$ is defined by

$$\bar{\epsilon}^{(s)} = \frac{|e^{(1)}|\epsilon^{(e^{(1)})} + |e^{(2)}|\epsilon^{(e^{(2)})}}{|e^{(1)}| + |e^{(2)}|}, \quad (2.3)$$

where $e^{(1)}$ and $e^{(2)}$ are the elements in \mathcal{T}_h sharing the edge corresponding to s , and $\epsilon^{(e^{(1)})}$ and $\epsilon^{(e^{(2)})}$ were defined in (2.1). The local smoothed gradient in (2.3) can also be expressed in a matrix-vector form as

$$\bar{\epsilon}^{(s)} = \bar{B}_{ES}^{(s)} \bar{u}^{(s)} \quad \text{with} \quad \bar{B}_{ES}^{(s)} = \frac{|e^{(1)}|}{|e^{(1)}| + |e^{(2)}|} B^{(e_1)} R^{(e_1)} + \frac{|e^{(2)}|}{|e^{(1)}| + |e^{(2)}|} B^{(e_2)} R^{(e_2)}, \quad \bar{u}^{(s)} = [u_1 \quad u_2 \quad u^{(1)} \quad u^{(2)}]^T, \quad (2.4)$$

where the vector $\bar{u}^{(s)}$ consists of the four degrees of freedom of $u \in V_h$ at the nodes of the elements sharing the edge corresponding to s as shown in Fig. 2(a), $B^{(e_1)}$ and $B^{(e_2)}$ were defined in (2.1), and $R^{(e_1)}$ and $R^{(e_2)}$ are boolean matrices that extract the degrees of freedom corresponding to the elements e_1 and e_2 , respectively, i.e.,

$$R^{(e_1)} = \begin{bmatrix} 1 & 0 & 0 & 0 \\ 0 & 1 & 0 & 0 \\ 0 & 0 & 1 & 0 \end{bmatrix}, \quad R^{(e_2)} = \begin{bmatrix} 1 & 0 & 0 & 0 \\ 0 & 1 & 0 & 0 \\ 0 & 0 & 0 & 1 \end{bmatrix}.$$

Finally, the stiffness matrix \bar{K}_{ES} for the ES-FEM can be obtained as

$$u^T \bar{K}_{ES} v = \int_{\Omega} \bar{\nabla}_{ES} u \cdot \bar{\nabla}_{ES} v \, d\Omega = \sum_{s \in \mathcal{S}_{h,ES}} |s| \left(\bar{B}_{ES}^{(s)} \bar{u}^{(s)} \right)^T \left(\bar{B}_{ES}^{(s)} \bar{v}^{(s)} \right), \quad u, v \in V_h, \quad (2.5)$$

where $\bar{\nabla}_{ES}$ denotes the global smoothed gradient operator corresponding to (2.3). It is known that the ES-FEM generally has the best predictive capability among the S-FEMs [4].

2.3. Strain-smoothed element method

When the SSE method is employed, a smoothed gradient field is constructed for each element in \mathcal{T}_h , and the gradient information in all elements adjacent to a target element is utilized. No smoothing domains are required, that is, the domain discretization with the SSE method is the same as the one with the standard FEM.

For an element $e \in \mathcal{T}_h$, there can be up to three neighboring elements in \mathcal{T}_h through element edges, say $e^{(k)}$, $1 \leq k \leq 3$. An intermediate smoothed gradient $\hat{\epsilon}^{(k)}$ between e and its neighboring element $e^{(k)}$ is defined by

$$\hat{\epsilon}^{(k)} = \frac{|e|\epsilon^{(e)} + |e^{(k)}|\epsilon^{(e^{(k)})}}{|e| + |e^{(k)}|}, \quad (2.6)$$

where $\epsilon^{(e)}$ and $\epsilon^{(e^{(k)})}$ were defined in (2.1). If there is no adjacent element $e^{(k)}$ for some k , then we simply use $\hat{\epsilon}^{(k)} = \epsilon^{(e)}$. Then, we construct a linear smoothed gradient field $\bar{\epsilon}^{(e)}$ on the target element e by unifying the intermediate smoothed gradients in (2.6). The values are assigned at three Gaussian integration points Gk , $1 \leq k \leq 3$, of e as the pointwise values of $\bar{\epsilon}^{(e)}$ as follows:

$$\bar{\epsilon}^{(e)}(Gk) = \frac{\hat{\epsilon}^{(k-1)} + \hat{\epsilon}^{(k)}}{2}, \quad (2.7)$$

with the convention $\hat{\epsilon}^{(0)} = \hat{\epsilon}^{(3)}$. The smoothed gradient field $\bar{\epsilon}^{(e)}$ is uniquely determined within e by linear interpolation of the pointwise values. The local smoothed gradient in (2.7) can be expressed in a matrix-vector form as

$$\bar{\epsilon}^{(e)} = \bar{B}_{\text{SSE}}^{(e)} \bar{u}^{(e)} \quad \text{with} \quad \bar{B}_{\text{SSE}}^{(e)} = \frac{1}{2} \begin{bmatrix} \bar{B}_{\text{ES}}^{(s_1)} R^{(s_1)} + \bar{B}_{\text{ES}}^{(s_3)} R^{(s_3)} \\ \bar{B}_{\text{ES}}^{(s_1)} R^{(s_1)} + \bar{B}_{\text{ES}}^{(s_2)} R^{(s_2)} \\ \bar{B}_{\text{ES}}^{(s_2)} R^{(s_2)} + \bar{B}_{\text{ES}}^{(s_3)} R^{(s_3)} \end{bmatrix}, \quad \bar{u}^{(e)} = [u_1 \quad u_2 \quad u_3 \quad u^{(1)} \quad u^{(2)} \quad u^{(3)}]^T, \quad (2.8)$$

where the vector $\bar{\epsilon}^{(e)}$ comprises three pointwise values $\bar{\epsilon}^{(e)}(G1)$, $\bar{\epsilon}^{(e)}(G2)$, and $\bar{\epsilon}^{(e)}(G3)$, the vector $\bar{u}^{(e)}$ consists of at most six degrees of freedom of $u \in V_h$ at the nodes of e and its neighboring elements (see Fig. 2(b)), the matrices $\bar{B}_{\text{ES}}^{(s_k)}$, $1 \leq k \leq 3$, were defined in (2.4), and $R^{(s_k)}$ are boolean matrices that extract the degrees of freedom corresponding to the subdomains s_k , i.e.,

$$R^{(s_1)} = \begin{bmatrix} 1 & 0 & 0 & 0 & 0 & 0 \\ 0 & 1 & 0 & 0 & 0 & 0 \\ 0 & 0 & 0 & 1 & 0 & 0 \\ 0 & 0 & 1 & 0 & 0 & 0 \end{bmatrix}, \quad R^{(s_2)} = \begin{bmatrix} 0 & 1 & 0 & 0 & 0 & 0 \\ 0 & 0 & 1 & 0 & 0 & 0 \\ 0 & 0 & 0 & 0 & 1 & 0 \\ 1 & 0 & 0 & 0 & 0 & 0 \end{bmatrix}, \quad R^{(s_3)} = \begin{bmatrix} 0 & 0 & 1 & 0 & 0 & 0 \\ 1 & 0 & 0 & 0 & 0 & 0 \\ 0 & 0 & 0 & 0 & 0 & 1 \\ 0 & 1 & 0 & 0 & 0 & 0 \end{bmatrix}.$$

In the SSE method, the smoothed gradient field is constructed for each element in \mathcal{T}_h , and consequently, numerical integration is performed on the element as in the standard FEM (2.2). More precisely, the stiffness matrix \bar{K}_{SSE} for the SSE method is calculated by

$$u^T \bar{K}_{\text{SSE}} v = \int_{\Omega} \bar{\nabla}_{\text{SSE}} u \cdot \bar{\nabla}_{\text{SSE}} v \, d\Omega = \sum_{e \in \mathcal{T}_h} \frac{|e|}{3} \left(\bar{B}_{\text{SSE}}^{(e)} \bar{u}^{(e)} \right)^T \left(\bar{B}_{\text{SSE}}^{(e)} \bar{v}^{(e)} \right), \quad u, v \in V_h, \quad (2.9)$$

where $\bar{\nabla}_{\text{SSE}}$ denotes the global smoothed gradient operator corresponding to (2.7).

The strain-smoothed elements adopting the SSE method have been verified to pass the three basic tests (zero energy mode, isotropic element, and patch tests) and show more improved convergence behaviors compared with other competitive elements in various numerical problems [10, 11, 12].

3. Spectral equivalence among stiffness matrices

In this section, we prove that the stiffness matrices of the ES-FEM and SSE method defined in (2.5) and (2.9), respectively, are spectrally equivalent to that of the standard FEM defined in (2.2). The results of this section imply that the ES-FEM and SSE method can adopt any preconditioner designed for the standard FEM without degrading the performance of the preconditioner. In this sense, they are advantageous for use with preconditioned iterative schemes such as the preconditioned conjugate gradient method and other Krylov space methods [16] compared to other FEMs with strain smoothing. On the contrary, in Section 6, we will show that the stiffness matrix of the NS-FEM is not spectrally equivalent to that of the standard FEM in general.

We first present a simple but useful lemma that is required for the spectral analysis of the ES-FEM and SSE method.

Lemma 3.1. *Let ω_1 and ω_2 be polygonal regions in \mathbb{R}^2 sharing an edge f , i.e., $\bar{\omega}_1 \cap \bar{\omega}_2 = f$. If a continuous and piecewise linear function $u: \omega_1 \cup \omega_2 \rightarrow \mathbb{R}$ satisfies $w_1 \nabla u|_{\omega_1} + w_2 \nabla u|_{\omega_2} = 0$ for some $w_1, w_2 > 0$, then it is constant along f .*

Proof. Let t be a unit vector along the direction of the edge f . If we suppose that u is not constant along f , then it follows that $\nabla u|_{\omega_1} \cdot t = \nabla u|_{\omega_2} \cdot t \neq 0$. However, it contradicts $(w_1 \nabla u|_{\omega_1} + w_2 \nabla u|_{\omega_2}) \cdot t = 0$. \square

Using Lemma 3.1 and the fact that the strain smoothing operation of the ES-FEM is an orthogonal projection in $(L^2(\Omega))^2$ [9], we can prove the spectral equivalence between the stiffness matrices of the standard FEM and ES-FEM as follows.

Theorem 3.2. *The stiffness matrices K and \bar{K}_{ES} of the standard FEM and ES-FEM defined in (2.2) and (2.5), respectively, are spectrally equivalent. That is, there exists two positive constants \underline{C} and \bar{C} independent of the mesh size h such that*

$$\underline{C} u^T K u \leq u^T \bar{K}_{\text{ES}} u \leq \bar{C} u^T K u \quad \forall u \in V_h.$$

Proof. Since the strain smoothing operation of the ES-FEM is an $(L^2(\Omega))^2$ -orthogonal projection [9, Remark 4], it follows that

$$u^T \bar{K}_{\text{ES}} u = \int_{\Omega} |\bar{\nabla}_{\text{ES}} u|^2 d\Omega \leq \int_{\Omega} |\nabla u|^2 d\Omega = u^T K u \quad \forall u \in V_h.$$

Consequently, we have $\bar{C} = 1$. Next, we estimate \underline{C} . For any interior element $e \in \mathcal{T}_h$ and its adjacent elements $e^{(k)} \in \mathcal{T}_h$, $1 \leq k \leq 3$, we have

$$\int_e |\bar{\nabla}_{\text{ES}} u|^2 d\Omega = \sum_{k=1}^3 \int_{e \cap s^{(k)}} |\bar{\nabla}_{\text{ES}} u|^2 d\Omega = \frac{|e|}{3} \sum_{k=1}^3 (\hat{\epsilon}^{(k)})^T \hat{\epsilon}^{(k)},$$

where $s^{(k)}$ is the smoothing domain corresponding to the edge shared by e and $e^{(k)}$, and $\hat{\epsilon}^{(k)}$ was given in (2.6). In order for $\int_e |\bar{\nabla}_{\text{ES}} u|^2 d\Omega$ to be zero, we must have $\hat{\epsilon}^{(k)} = 0$ for all k . Then by Lemma 3.1, u is constant along all the edges of e , so that u is constant on e and

$$\int_e |\nabla u|^2 d\Omega = |e| (\epsilon^{(e)})^T \epsilon^{(e)} = 0,$$

where $\epsilon^{(e)}$ was defined in (2.1). Up to this point, we have shown that

$$\int_e |\bar{\nabla}_{\text{ES}} u|^2 d\Omega = 0 \quad \text{implies} \quad \int_e |\nabla u|^2 d\Omega = 0.$$

Hence there exists a positive constant C_e such that

$$\int_e |\bar{\nabla}_{\text{ES}} u|^2 d\Omega \geq C_e \int_e |\nabla u|^2 d\Omega \quad \forall u \in V_h. \quad (3.1)$$

One can easily verify by the usual scaling argument that C_e is independent of the mesh size h and depends only on geometries of e and $e^{(k)}$. Similar arguments can be used to obtain an estimate of the form (3.1) for the case of boundary elements; we omit details. Since \mathcal{T}_h is quasi-uniform, the constant C_e in (3.1) has a uniform positive lower bound, say \underline{C} , over all $e \in \mathcal{T}_h$. Then for any $u \in V_h$, we have

$$u^T \bar{K}_{\text{ES}} u = \sum_{e \in \mathcal{T}_h} \int_e |\bar{\nabla}_{\text{ES}} u|^2 d\Omega \geq \underline{C} \sum_{e \in \mathcal{T}_h} \int_e |\nabla u|^2 d\Omega = \underline{C} u^T K u,$$

which completes the proof. \square

A useful consequence of Theorem 3.2 is that any preconditioner for the standard FEM works for the ES-FEM as well. Corollary 3.3 presents a rigorous statement on the performance of a preconditioner applied to the ES-FEM. Note that, for a symmetric and positive definite matrix A , $\kappa(A)$ denotes the condition number of A , i.e.,

$$\kappa(A) = \frac{\lambda_{\max}(A)}{\lambda_{\min}(A)},$$

where $\lambda_{\min}(A)$ and $\lambda_{\max}(A)$ are the minimum and maximum eigenvalues of A , respectively.

Corollary 3.3. *Any preconditioner M^{-1} for the standard FEM $Ku = f$ works for the ES-FEM $\bar{K}_{\text{ES}}u = f$ as well. More precisely, there exists a positive constant C independent of the mesh size h such that*

$$\kappa(M^{-1}\bar{K}_{\text{ES}}) \leq C\kappa(M^{-1}K).$$

Proof. By [21, Corollary C.2], it follows that

$$\kappa(M^{-1}\bar{K}_{\text{ES}}) \leq \kappa(K^{-1}\bar{K}_{\text{ES}})\kappa(M^{-1}K) \leq \frac{\bar{C}}{\underline{C}}\kappa(M^{-1}K),$$

where \underline{C} and \bar{C} were given in Theorem 3.2. Setting $C = \bar{C}/\underline{C}$ completes the proof. \square

Here, we provide a detailed explanation for Corollary 3.3. Suppose that we have a preconditioner M^{-1} for the standard FEM such that $\kappa(M^{-1}K) = O(h^{-\alpha})$ for some $\alpha \geq 0$. Then, Corollary 3.3 implies that preconditioning the stiffness matrix of the ES-FEM by M^{-1} yields the same condition number estimate as the standard FEM, i.e., $\kappa(M^{-1}\bar{K}_{\text{ES}}) = O(h^{-\alpha})$. Therefore, it is ensured that any preconditioned iterative scheme for the ES-FEM reaches a target accuracy within the same number of iterations up to a multiplicative constant as the case of the standard FEM.

Similar results can be obtained for the SSE method as well. The spectral equivalence between the stiffness matrices of the standard FEM and SSE method can be deduced by invoking the fact that the strain smoothing step of the SSE method can be represented as a composition of orthogonal projection operators among some assumed strain spaces [13].

Theorem 3.4. *The stiffness matrices K and \bar{K}_{SSE} of the standard FEM and SSE method defined in (2.2) and (2.9), respectively, are spectrally equivalent. That is, there exists two positive constants \underline{C} and \bar{C} independent of the mesh size h such that*

$$\underline{C}u^T Ku \leq u^T \bar{K}_{\text{SSE}}u \leq \bar{C}u^T Ku, \quad u \in V_h.$$

Proof. Note that the strain smoothing operation of the SSE method can be regarded as a composition of $(L^2(\Omega))^2$ -orthogonal projections [13, Theorem 3.3]. Hence, we deduce that $u^T \bar{K}_{\text{SSE}}u \leq u^T Ku$ for all $u \in V_h$, i.e., $\bar{C} = 1$. In order to prove the \underline{C} -inequality, it suffices to show that

$$\int_e |\bar{\nabla}_{\text{SSE}}u|^2 d\Omega = 0 \quad \text{implies} \quad \int_e |\nabla u|^2 d\Omega = 0 \quad (3.2)$$

for any $e \in \mathcal{T}_h$; if we show (3.2), then one can deduce the \underline{C} -inequality by the same argument as in Theorem 3.2. We take an interior element $e \in \mathcal{T}_h$ and suppose that $\int_e |\bar{\nabla}_{\text{SSE}}u|^2 d\Omega = 0$; the case of boundary elements can be shown in a similar manner. Observing that

$$\int_e |\bar{\nabla}_{\text{SSE}}u|^2 d\Omega = \frac{|e|}{3} \sum_{k=1}^3 \left(\frac{\hat{\epsilon}^{(k-1)} + \hat{\epsilon}^{(k)}}{2} \right)^T \left(\frac{\hat{\epsilon}^{(k-1)} + \hat{\epsilon}^{(k)}}{2} \right),$$

where $\hat{\epsilon}^{(k)}$ was defined in (2.6), we have $\hat{\epsilon}^{(k-1)} + \hat{\epsilon}^{(k)} = 0$ for all k . Equivalently, we get $\hat{\epsilon}^{(k)} = 0$ for all k . Invoking Lemma 3.1, we deduce that u is constant on e so that $\int_e |\nabla u|^2 d\Omega = 0$. Therefore, (3.2) holds. \square

The following corollary is a direct consequence of Theorem 3.4; it says that any preconditioner for the standard FEM is also well-suited for the SSE method. Derivation of Corollary 3.5 can be done in the same way as Corollary 3.3.

Corollary 3.5. *Any preconditioner M^{-1} for the standard FEM $Ku = f$ works for the SSE method $\bar{K}_{\text{SSE}}u = f$ as well. More precisely, there exists a positive constant C independent of the mesh size h such that*

$$\kappa(M^{-1}\bar{K}_{\text{SSE}}) \leq C\kappa(M^{-1}K).$$

We present another useful consequence of Theorems 3.2 and 3.4: a Poincaré–Friedrichs-type inequality for the ES-FEM and SSE method. Poincaré–Friedrichs-type inequalities are especially useful for convergence analysis of FEMs with strain smoothing; see, e.g., [9, 13].

Proposition 3.6. *Let $\bar{\nabla}$ denote the smoothed gradient operator for either the ES-FEM or SSE method. Then, there exists a positive constant C independent of the mesh size h such that*

$$\int_{\Omega} |\bar{\nabla} u|^2 d\Omega \geq C \int_{\Omega} u^2 d\Omega, \quad u \in V_h.$$

Proof. Combining the standard Poincaré–Friedrichs inequality [21, Lemma A.14] with Theorems 3.2 and 3.4 yields the desired result. \square

Remark 3.7. Proposition 3.6 means that the bilinear form

$$\bar{a}(u, v) = \int_{\Omega} \bar{\nabla} u \cdot \bar{\nabla} v d\Omega, \quad u, v \in V_h$$

is coercive. Coercivity of the bilinear form $\bar{a}(\cdot, \cdot)$ corresponding to the S-FEMs was first proven in [28] using a positivity relay argument. We note that the coercivity constant C in Proposition 3.6 is proven to be independent of h , whereas that in [28] was not. That is, Proposition 3.6 provides a sharper result than [28].

4. Improvement of preconditioners

As we observed in Section 3, existing preconditioners for the standard FEM can be applied to the ES-FEM and SSE method, inheriting good convergence properties from the case of the standard FEM. Meanwhile, when applied to the ES-FEM and SSE method, the performance of preconditioners based on subspace correction [25, 26] can be further improved by modifying local solvers appropriately. In this section, we present how to construct improved subspace correction preconditioners for the ES-FEM and SSE method. Specifically, we propose some two-level additive Schwarz preconditioners [21] for the ES-FEM and SSE method; note that Schwarz preconditioning is a standard methodology of parallel computing for large-scale finite element problems; see, e.g., [22, 23, 24]. Although we deal with two-level additive Schwarz preconditioner as descriptive examples, the method of improvement introduced in this section can be applied to various subspace correction preconditioners such as multigrid and domain decomposition preconditioners. Throughout this section, we omit the subscript h standing for the mesh size if there is no ambiguity.

4.1. Two-level additive Schwarz preconditioner

We first summarize key features of the standard two-level additive Schwarz preconditioner for the standard FEM [21]. Assuming that the domain Ω admits a coarse triangulation \mathcal{T}_H with the maximal element diameter H , it is decomposed into \mathcal{N} nonoverlapping subdomains $\{\Omega_j\}_{j=1}^{\mathcal{N}}$ such that each Ω_j is the union of several coarse elements in \mathcal{T}_h , and the number of coarse elements consisting of Ω_j is uniformly bounded. Then, each Ω_j is enlarged to form a larger region Ω'_j by adding layers of fine elements with the overlap width δ . If we set

$$V_j = \{v_j \in H_0^1(\Omega'_j) : v_j|_e \in \mathcal{P}_1(e) \forall e \in \mathcal{T}_h \text{ inside } \Omega'_j\}, \quad 1 \leq j \leq \mathcal{N},$$

and

$$V_0 = \{v_0 \in H_0^1(\Omega) : v_0|_e \in \mathcal{P}_1(e) \forall e \in \mathcal{T}_H\},$$

then $\{V_j\}_{j=0}^{\mathcal{N}}$ forms a space decomposition of $V = V_h$, i.e.,

$$V = \sum_{j=0}^{\mathcal{N}} R_j^T V_j,$$

where $R_j^T: V_j \rightarrow V$, $0 \leq j \leq \mathcal{N}$, is the natural interpolation operator. In this setting, the standard two-level additive Schwarz preconditioner is given by

$$M^{-1} = \sum_{j=0}^{\mathcal{N}} R_j^T K_j^{-1} R_j, \quad (4.1)$$

where $K_j: V_j \rightarrow V_j$, $0 \leq j \leq \mathcal{N}$, is the local stiffness matrix on the subspace V_j , i.e., $K_j = R_j K R_j^T$. It is well-known that the additive Schwarz condition number (see (A.1)) of the preconditioned operator $M^{-1}K$ satisfies the following upper bound [21, Theorem 3.13].

Proposition 4.1. *Let M^{-1} be the two-level additive Schwarz preconditioner defined in (4.1). Then it satisfies that*

$$\kappa_{\text{ASM}}(M^{-1}K) \leq C \left(1 + \frac{H}{\delta}\right),$$

where κ_{ASM} denotes the additive Schwarz condition number defined in (A.1) and C is a positive constant independent of h , H , and δ .

Proposition 4.1 can be proven by using the abstract convergence theory of additive Schwarz methods presented in [21, 29]; see Appendix A for a brief summary. Combining Corollaries 3.3 and 3.5 with Proposition 4.1, we deduce that the preconditioner M^{-1} works for the ES-FEM and SSE method as well as for the standard FEM.

Corollary 4.2. *Let M^{-1} be the two-level additive Schwarz preconditioner defined in (4.1) and let \bar{K} be the stiffness matrix of either the ES-FEM or SSE method. Then it satisfies that*

$$\kappa_{\text{ASM}}(M^{-1}\bar{K}) \leq C \left(1 + \frac{H}{\delta}\right),$$

where κ_{ASM} denotes the additive Schwarz condition number defined in (A.1) and C is a positive constant independent of h , H , and δ .

Corollary 4.2 means that preconditioning the ES-FEM and SSE method by M^{-1} shares advantages with preconditioning the standard FEM by M^{-1} . For instance, the M^{-1} -preconditioned SSE method is scalable in the sense that its condition number does not deteriorate even if the fine mesh size h decreases when the coarse mesh size H and the overlap width δ decrease keeping H/δ and δ/h constant. Therefore, the M^{-1} -preconditioned SSE method is suitable for large-scale parallel computing in a way that each subspace V_j is assigned to a processor; such an aspect is a usual advantage of subspace correction methods as parallel numerical solvers [21].

4.2. Enhanced local problems

Until now, we have observed that subspace correction preconditioners designed for the standard FEM do their roles properly even if they are applied to the ES-FEM and SSE method. Meanwhile, it is possible to modify the preconditioners adaptively to them to have even better performance. The idea is straightforward; we simply replace the local stiffness matrices in (4.1) defined in terms of the standard FEM by those defined in terms of either the ES-FEM or SSE method. Let $\bar{K}: V \rightarrow V$ be the stiffness matrix of either the ES-FEM or SSE method. We set

$$\bar{M}^{-1} = \sum_{j=0}^N R_j^T \bar{K}_j^{-1} R_j, \quad (4.2)$$

where $\bar{K}_j: V_j \rightarrow V_j$, $0 \leq j \leq N$, is defined by $\bar{K}_j = R_j \bar{K} R_j^T$. That is, \bar{K}_j is the local stiffness matrix of either the ES-FEM or SSE method on the subspace V_j . Invoking Theorem Appendix A.4, we can mathematically explain why the preconditioner \bar{M}^{-1} performs better than M^{-1} when it is applied to either the ES-FEM or SSE method. Theorem 4.3 says that \bar{M}^{-1} is a better preconditioner for \bar{K} than M^{-1} , and it inherits good properties of M^{-1} such as the scalability.

Theorem 4.3. *The enhanced additive Schwarz preconditioner \bar{M}^{-1} defined in (4.2) performs better than the original additive Schwarz preconditioner M^{-1} defined in (4.1). More precisely, it satisfies that*

$$\kappa_{\text{ASM}}(\bar{M}^{-1}\bar{K}) \leq \kappa_{\text{ASM}}(M^{-1}\bar{K}),$$

where \bar{K} is the stiffness matrix of either the ES-FEM or SSE method, and κ_{ASM} denotes the additive Schwarz condition number defined in (A.1).

Proof. By the definition of κ_{ASM} , it suffices to show that

$$\omega_0(\bar{M}^{-1}\bar{K})C_0^2(\bar{M}^{-1}\bar{K}) \leq \omega_0(M^{-1}\bar{K})C_0^2(M^{-1}\bar{K}), \quad \tau_0(\bar{M}^{-1}\bar{K}) \geq \tau_0(M^{-1}\bar{K}),$$

where C_0 , τ_0 , and ω_0 are defined in Assumptions Appendix A.1, Appendix A.2, and Appendix A.3, respectively. First, we readily get $\tau_0(\bar{M}^{-1}\bar{K}) = \tau_0(M^{-1}\bar{K})$ because Assumption Appendix A.2 does not rely on which local operators

are used. Since $\bar{K}_j = R_j \bar{K} R_j^T$, $0 \leq j \leq N$, it follows by the definition of ω_0 that $\omega_0(\bar{M}^{-1} \bar{K}) = 1$. Meanwhile, as the inequality

$$v_j^T \bar{K}_j v_j \leq \lambda_{\max}(K_j^{-1} \bar{K}_j) v_j^T K_j v_j \quad \forall v_j \in V_j$$

is sharp for all $0 \leq j \leq N$, we get

$$\omega_0(M^{-1} \bar{K}) = \max_{0 \leq j \leq N} \lambda_{\max}(K_j^{-1} \bar{K}_j).$$

Next, we take any $v \in V$ and let $v = \sum_{j=0}^N R_j^T v_j$ be a decomposition of v such that

$$\sum_{j=0}^N v_j^T K_j v_j = C_0^2(M^{-1} \bar{K}) v^T \bar{K} v.$$

For the existence of such a decomposition, one may refer to [21, Lemma 2.5]. Then it follows that

$$\sum_{j=0}^N v_j^T \bar{K}_j v_j \leq \sum_{j=0}^N \lambda_{\max}(K_j^{-1} \bar{K}_j) v_j^T K_j v_j \leq \omega_0(M^{-1} \bar{K}) \sum_{j=0}^N v_j^T K_j v_j = \omega_0(M^{-1} \bar{K}) C_0^2(M^{-1} \bar{K}) v^T \bar{K} v,$$

which implies $C_0^2(\bar{M}^{-1} \bar{K}) \leq \omega_0(M^{-1} \bar{K}) C_0^2(M^{-1} \bar{K})$ by the definition of C_0 . Consequently, we have

$$\omega_0(\bar{M}^{-1} \bar{K}) C_0^2(\bar{M}^{-1} \bar{K}) = C_0^2(\bar{M}^{-1} \bar{K}) \leq \omega_0(M^{-1} \bar{K}) C_0^2(M^{-1} \bar{K}),$$

which completes the proof. \square

We conclude this section by introducing a variant of (4.2) that is more convenient to implement. When we implement (4.2), a cumbersome step is an assemblage of the coarse stiffness matrix $\bar{K}_0 = R_0 \bar{K} R_0^T$. While the interpolation operator R_0^T is defined for functions in the coarse space V_0 , the strain smoothing procedure in \bar{K} is defined in the fine-scale space V . Hence, to assemble \bar{K}_0 , we need some fine-scale computations although it acts on the coarse space V_0 . For the sake of avoiding such computations, we propose the following alternative two-level additive Schwarz preconditioner:

$$\bar{M}_{\text{alt}}^{-1} = R_0^T K_0^{-1} R_0 + \sum_{j=1}^N R_j^T \bar{K}_j^{-1} R_j. \quad (4.3)$$

The alternative preconditioner $\bar{M}_{\text{alt}}^{-1}$ involves the stiffness matrices of the strain smoothing methods in the fine-scale subspaces, whereas its coarse-scale operation is defined in terms of the standard FEM. Therefore, it is easier to implement than \bar{M}^{-1} . As $\bar{M}_{\text{alt}}^{-1}$ is a kind of a hybrid of M^{-1} and \bar{M}^{-1} , it is expected that the convergence behavior of the $\bar{M}_{\text{alt}}^{-1}$ -preconditioned operator lies between those of the M^{-1} - and \bar{M}^{-1} -preconditioned operators. Numerical comparisons among the preconditioners M^{-1} , \bar{M}^{-1} , and $\bar{M}_{\text{alt}}^{-1}$ will be presented in Section 5.

5. Numerical results

In this section, we verify the theoretical results presented so far through numerical experiments. We solve two-dimensional Poisson and linear elasticity problems using three-node triangular elements with the ES-FEM and SSE method. The preconditioned conjugate gradient method is used for solving a linear system of equations with a stop criterion of 10^{-10} percent on the relative residual, and with zero initial guess. We verify the spectral equivalence among the stiffness matrices of the standard FEM, ES-FEM, and SSE method. Also, we compare the performance of the two-level additive Schwarz preconditioners M^{-1} , \bar{M}^{-1} , and $\bar{M}_{\text{alt}}^{-1}$ introduced in (4.1), (4.2), and (4.3), respectively.

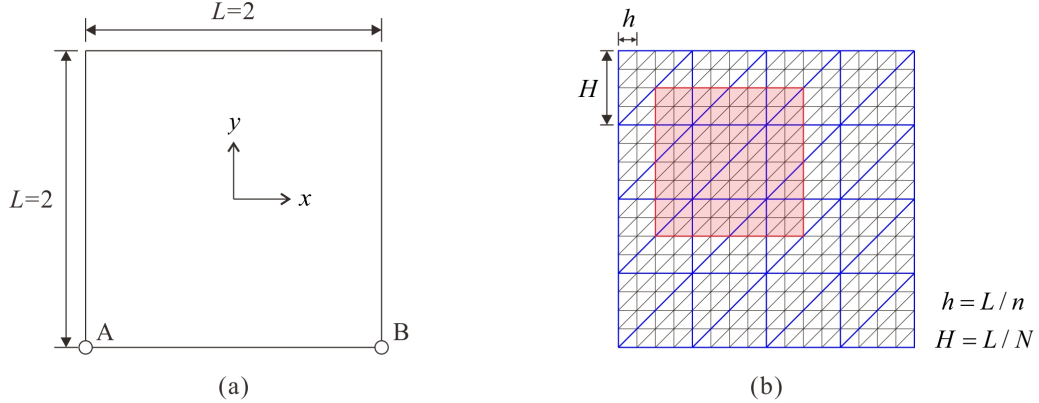


Figure 3: **(a)** Square domain $\Omega = (-1, 1)^2 \subset \mathbb{R}^2$ for the model Poisson and linear elasticity problems. **(b)** Domain decomposition setting when $n = 2^4, N = 2^2$, and $\delta = 2h$.

	$n = 2^3$	$n = 2^4$	$n = 2^5$	$n = 2^6$	$n = 2^7$
ES-FEM	1.90e0	2.04e0	2.07e0	2.08e0	2.09e0
SSE	2.87e0	3.24e0	3.34e0	3.37e0	3.38e0

Table 1: Condition numbers $\kappa(K^{-1}\bar{K}_{\text{ES}})$ and $\kappa(K^{-1}\bar{K}_{\text{SSE}})$ for the model Poisson problem (5.1).

5.1. Poisson equation

The first example is the Poisson problem defined on the domain $\Omega = (-1, 1)^2 \subset \mathbb{R}^2$ shown in Fig. 3(a):

$$\begin{aligned} -\Delta u &= f & \text{in } \Omega, \\ u &= 0 & \text{on } \partial\Omega, \end{aligned} \quad (5.1)$$

where the function f is given such that the problem has the exact solution $u(x, y) = e^{8(x+y)} \sin(\pi x) \sin(\pi y)$. For discretization of the square domain Ω of side length $L = 2$, we employ the standard checkerboard-type triangulations \mathcal{T}_h with $2 \times n \times n$ fine elements ($n = 2^3, 2^4, \dots, 2^7$) and \mathcal{T}_H with $2 \times N \times N$ coarse elements ($N = 2, 2^2, \dots, 2^5$). Each subdomain Ω_j , $1 \leq j \leq N = N \times N$, is a square region composed of two coarse elements. The sizes of the fine and coarse meshes are calculated by $h = L/n$ and $H = L/N$, respectively; see Fig. 3(b) for the case of $n = 2^4$ and $N = 2^2$. We set the overlap width δ as $2h$, so that δ/h is constant.

Table 1 provides the condition numbers $\kappa(K^{-1}\bar{K}_{\text{ES}})$ and $\kappa(K^{-1}\bar{K}_{\text{SSE}})$ for various values of n . The condition numbers $\kappa(K^{-1}\bar{K}_{\text{ES}})$ and $\kappa(K^{-1}\bar{K}_{\text{SSE}})$ do not increase even if n gets larger. Hence, we can deduce that the stiffness matrices \bar{K}_{ES} and \bar{K}_{SSE} of the ES-FEM and SSE method, respectively, are spectrally equivalent to the stiffness matrix K of the standard FEM. This numerically verifies Theorems 3.2 and 3.4. Table 2 shows the condition numbers of the M^{-1} -, \bar{M}^{-1} -, and $\bar{M}_{\text{alt}}^{-1}$ -preconditioned stiffness matrices of the ES-FEM and the corresponding conjugate gradient iteration counts denoted as #iter with respect to various values of n and N . As we have explained theoretically in Section 4, M^{-1} -, \bar{M}^{-1} -, and $\bar{M}_{\text{alt}}^{-1}$ -preconditioned ES-FEMs are all numerically scalable in the sense that both the condition number and the number of iterations do not increase when n and N increase keeping n/N constant. Moreover, we can observe that each iteration count for the preconditioner \bar{M}^{-1} is less than the corresponding counterpart for the preconditioner M^{-1} , which numerically verifies Theorem 4.3. We also highlight that the condition numbers and iteration counts for the preconditioner $\bar{M}_{\text{alt}}^{-1}$ are comparable to those for \bar{M}^{-1} . Hence, as we have claimed in Section 4, $\bar{M}_{\text{alt}}^{-1}$ can be a good alternative to \bar{M}^{-1} with the comparable performance and easy implementation. Table 3 provides the condition numbers and the iteration counts #iter of the preconditioned SSE methods; similar discussions to the case of Table 2 can be made for Table 3. Fig. 4 depicts the condition numbers of the $\bar{M}_{\text{alt}}^{-1}$ -preconditioned ES-FEM and SSE method when $n/N (= H/h)$ is fixed as 4. One can readily observe that the condition numbers of the $\bar{M}_{\text{alt}}^{-1}$ -preconditioned methods remain almost the same when both h and H decrease keeping their ratio H/h constant.

Precond.	N	$n = 2^3$		$n = 2^4$		$n = 2^5$		$n = 2^6$		$n = 2^7$	
		#iter	κ	#iter	κ	#iter	κ	#iter	κ	#iter	κ
None		17	1.73e1	34	6.92e1	69	2.77e2	138	1.11e3	278	4.43e3
M^{-1}	2	13	5.73e0	14	6.67e0	13	6.41e0	14	7.99e0	15	1.52e1
	2^2	-	-	16	5.98e0	17	6.63e0	17	6.91e0	21	1.07e1
	2^3	-	-	-	-	16	5.86e0	18	6.72e0	19	7.00e0
	2^4	-	-	-	-	-	-	18	6.00e0	19	6.76e0
	2^5	-	-	-	-	-	-	-	-	18	6.04e0
\bar{M}^{-1}	2	9	4.81e0	9	5.58e0	10	6.84e0	11	1.00e1	12	1.76e1
	2^2	-	-	14	5.45e0	14	5.88e0	15	6.98e0	20	1.20e1
	2^3	-	-	-	-	15	5.49e0	15	5.91e0	17	7.00e0
	2^4	-	-	-	-	-	-	16	5.50e0	16	5.91e0
	2^5	-	-	-	-	-	-	-	-	16	5.45e0
$\bar{M}_{\text{alt}}^{-1}$	2	9	4.75e0	9	5.62e0	9	6.88e0	11	1.00e1	12	1.76e1
	2^2	-	-	14	5.33e0	14	5.90e0	15	7.00e0	20	1.20e1
	2^3	-	-	-	-	15	5.37e0	15	5.95e0	16	7.00e0
	2^4	-	-	-	-	-	-	16	5.35e0	16	5.94e0
	2^5	-	-	-	-	-	-	-	-	16	5.24e0

Table 2: Condition numbers κ and iteration counts #iter of the ES-FEM applied to the model Poisson problem (5.1) with the two-level additive Schwarz preconditioners M^{-1} , \bar{M}^{-1} , and $\bar{M}_{\text{alt}}^{-1}$ defined in (4.1), (4.2), and (4.3), respectively.

Precond.	N	$n = 2^3$		$n = 2^4$		$n = 2^5$		$n = 2^6$		$n = 2^7$	
		#iter	κ	#iter	κ	#iter	κ	#iter	κ	#iter	κ
None		15	1.32e1	30	5.22e1	59	2.08e2	119	8.30e2	240	3.32e3
M^{-1}	2	14	7.16e0	16	9.49e0	16	9.55e0	15	9.30e0	16	1.40e1
	2^2	-	-	18	7.62e0	20	9.53e0	20	1.01e1	21	1.01e1
	2^3	-	-	-	-	19	7.72e0	20	9.47e0	22	1.03e1
	2^4	-	-	-	-	-	-	20	7.55e0	22	9.59e0
	2^5	-	-	-	-	-	-	-	-	21	7.74e0
\bar{M}^{-1}	2	9	4.77e0	9	5.48e0	9	6.73e0	10	9.49e0	12	1.67e1
	2^2	-	-	14	5.42e0	14	5.77e0	15	6.87e0	20	1.18e1
	2^3	-	-	-	-	15	5.46e0	15	5.79e0	16	6.87e0
	2^4	-	-	-	-	-	-	16	5.46e0	16	5.79e0
	2^5	-	-	-	-	-	-	-	-	16	5.43e0
$\bar{M}_{\text{alt}}^{-1}$	2	9	4.69e0	9	5.53e0	9	6.79e0	10	9.49e0	12	1.67e1
	2^2	-	-	14	5.27e0	14	5.80e0	15	6.90e0	20	1.18e1
	2^3	-	-	-	-	15	5.30e0	15	5.85e0	16	6.88e0
	2^4	-	-	-	-	-	-	16	5.29e0	16	5.84e0
	2^5	-	-	-	-	-	-	-	-	16	5.23e0

Table 3: Condition numbers κ and iteration counts #iter of the SSE method applied to the model Poisson problem (5.1) with the two-level additive Schwarz preconditioners M^{-1} , \bar{M}^{-1} , and $\bar{M}_{\text{alt}}^{-1}$ defined in (4.1), (4.2), and (4.3), respectively.

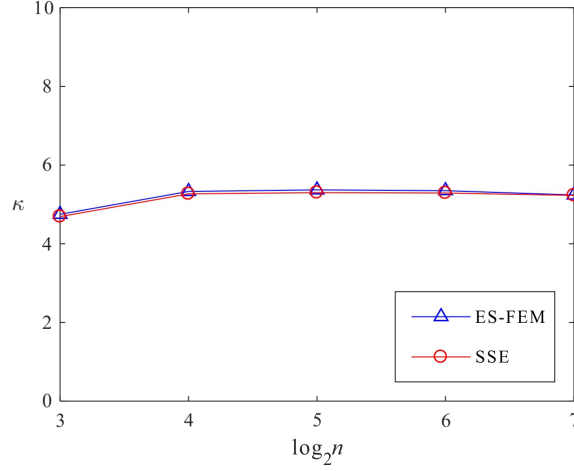


Figure 4: Condition numbers $\kappa(\bar{M}_{\text{alt}}^{-1}\bar{K})$ of the ES-FEM and SSE method applied to the model Poisson problem (5.1) when n varies and n/N ($= H/h$) is fixed as 4.

	$n = 2^3$	$n = 2^4$	$n = 2^5$	$n = 2^6$	$n = 2^7$
ES-FEM	2.27e0	2.30e0	2.32e0	2.33e0	2.33e0
SSE	3.68e0	3.78e0	3.84e0	3.86e0	3.87e0

Table 4: Condition numbers $\kappa(K^{-1}\bar{K}_{\text{ES}})$ and $\kappa(K^{-1}\bar{K}_{\text{SSE}})$ for the model linear elasticity problem (5.2).

5.2. Linear elasticity

Next, we consider the following model linear elasticity problem defined on the domain $\Omega = (-1, 1)^2 \subset \mathbb{R}^2$:

$$-\operatorname{div} \sigma(u) = b \quad \text{in } \Omega, \quad (5.2)$$

where $\sigma(u)$ is the Cauchy stress, b is the body force given by $b(x, y) = (-y^2, 1 - x^2)$, and the Dirichlet boundary condition $u = 0$ is given along line AB (see Fig. 3(a)). The plane stress condition is employed with Young's modulus $E = 1 \times 10^3$ and Poisson's ratio $\nu = 0.2$. The finite element models are constructed using $2 \times n \times n$ fine elements ($n = 2^3, 2^4, \dots, 2^7$), and $2 \times N \times N$ coarse elements ($N = 2, 2^2, \dots, 2^5$) with the overlap width $\delta = 2h$.

Table 4 gives the condition numbers $\kappa(K^{-1}\bar{K}_{\text{ES}})$ and $\kappa(K^{-1}\bar{K}_{\text{SSE}})$ for various n . Since the condition numbers for both of the ES-FEM and SSE method do not increase when n becomes larger, we can confirm the spectral equivalence among the stiffness matrices of the standard FEM, ES-FEM, and SSE method. Table 5 presents the condition numbers of the M^{-1} -, \bar{M}^{-1} -, and $\bar{M}_{\text{alt}}^{-1}$ -preconditioned stiffness matrices and the corresponding conjugate gradient iteration counts #iter for the ES-FEM, and Table 6 presents the results corresponding to the SSE method. Similar to the case of the Poisson problem, it is observed that both the number of iterations and the condition number do not increase when n and N grow keeping the ratio n/N constant, which implies that all the preconditioned methods are numerically scalable. Moreover, the numbers of iterations for the preconditioners \bar{M}^{-1} and $\bar{M}_{\text{alt}}^{-1}$ are smaller than the corresponding values for M^{-1} for most of the cases; this highlights the numerical efficiency of the proposed enhanced preconditioners \bar{M}^{-1} and $\bar{M}_{\text{alt}}^{-1}$ applied to the linear elasticity problem. Fig. 5 shows the condition numbers when the preconditioner $\bar{M}_{\text{alt}}^{-1}$ is used and n/N ($= H/h$) is fixed as 4 for the ES-FEM and SSE method. It is again observed that the condition numbers remain almost the same when the ratio H/h is constant. In conclusion, we have verified numerically that all the theoretical results developed in this paper are valid for both of the Poisson and linear elasticity problems.

6. Remarks on node-based strain smoothing

We observed that the ES-FEM and SSE method enjoy the spectral equivalence with the standard FEM. On the contrary, not every FEM with strain smoothing satisfies such equivalence property. In particular, we present an example that the stiffness matrix of the NS-FEM may not be spectrally equivalent to that of the standard FEM.

Precond.	N	$n = 2^3$		$n = 2^4$		$n = 2^5$		$n = 2^6$		$n = 2^7$	
		#iter	κ	#iter	κ	#iter	κ	#iter	κ	#iter	κ
None		71	1.05e3	139	3.71e3	272	1.38e4	535	5.32e4	1065	2.08e5
M^{-1}	2	21	8.80e0	22	9.73e0	24	1.16e1	30	1.76e1	40	3.14e1
	2^2	-	-	23	8.96e0	25	9.20e0	28	1.17e1	37	2.01e1
	2^3	-	-	-	-	23	8.33e0	25	9.20e0	28	1.19e1
	2^4	-	-	-	-	-	-	23	8.24e0	25	9.32e0
	2^5	-	-	-	-	-	-	-	-	23	8.16e0
\bar{M}^{-1}	2	18	7.66e0	20	9.26e0	22	1.22e1	28	1.94e1	38	3.51e1
	2^2	-	-	20	6.88e0	21	7.58e0	26	1.18e1	33	2.13e1
	2^3	-	-	-	-	20	6.83e0	22	8.58e0	26	1.19e1
	2^4	-	-	-	-	-	-	20	6.72e0	22	8.78e0
	2^5	-	-	-	-	-	-	-	-	20	6.71e0
$\bar{M}_{\text{alt}}^{-1}$	2	18	8.52e0	20	1.00e1	24	1.26e1	29	1.95e1	39	3.52e1
	2^2	-	-	21	7.77e0	23	9.25e0	28	1.24e1	36	2.17e1
	2^3	-	-	-	-	21	7.63e0	23	9.23e0	28	1.25e1
	2^4	-	-	-	-	-	-	21	7.60e0	24	9.50e0
	2^5	-	-	-	-	-	-	-	-	21	7.61e0

Table 5: Condition numbers κ and iteration counts #iter of the ES-FEM applied to the model linear elasticity problem (5.2) with the two-level additive Schwarz preconditioners M^{-1} , \bar{M}^{-1} , and $\bar{M}_{\text{alt}}^{-1}$ defined in (4.1), (4.2), and (4.3), respectively.

Precond.	N	$n = 2^3$		$n = 2^4$		$n = 2^5$		$n = 2^6$		$n = 2^7$	
		#iter	κ	#iter	κ	#iter	κ	#iter	κ	#iter	κ
None		67	8.00e2	123	2.80e3	237	1.04e4	464	3.99e4	922	1.56e5
M^{-1}	2	24	1.29e1	26	1.23e1	28	1.28e1	30	1.70e1	38	3.03e1
	2^2	-	-	27	1.43e1	28	1.32e1	29	1.36e1	36	1.96e1
	2^3	-	-	-	-	27	1.41e1	29	1.35e1	30	1.39e1
	2^4	-	-	-	-	-	-	27	1.33e1	30	1.36e1
	2^5	-	-	-	-	-	-	-	-	26	1.11e1
\bar{M}^{-1}	2	18	7.45e0	19	9.02e0	22	1.20e1	28	1.90e1	36	3.43e1
	2^2	-	-	20	6.76e0	21	7.34e0	25	1.15e1	33	2.08e1
	2^3	-	-	-	-	20	6.67e0	22	8.35e0	25	1.16e1
	2^4	-	-	-	-	-	-	20	6.55e0	22	8.55e0
	2^5	-	-	-	-	-	-	-	-	20	6.54e0
$\bar{M}_{\text{alt}}^{-1}$	2	18	8.33e0	20	9.82e0	23	1.24e1	29	1.91e1	37	3.44e1
	2^2	-	-	21	7.56e0	23	9.00e0	27	1.21e1	35	2.11e1
	2^3	-	-	-	-	21	7.25e0	23	8.99e0	27	1.22e1
	2^4	-	-	-	-	-	-	21	7.31e0	23	9.19e0
	2^5	-	-	-	-	-	-	-	-	21	7.32e0

Table 6: Condition numbers κ and iteration counts #iter of the SSE method applied to the model linear elasticity problem (5.2) with the two-level additive Schwarz preconditioners M^{-1} , \bar{M}^{-1} , and $\bar{M}_{\text{alt}}^{-1}$ defined in (4.1), (4.2), and (4.3), respectively.

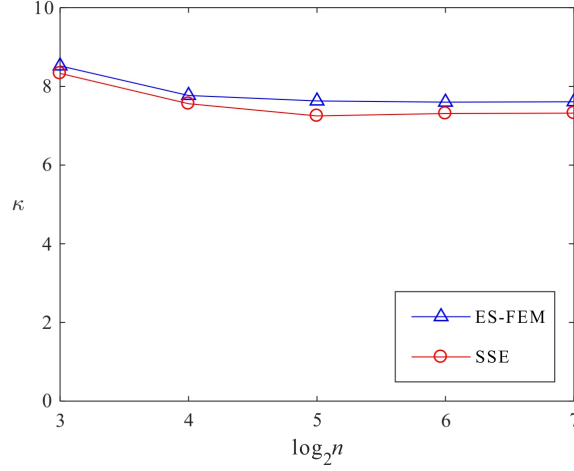


Figure 5: Condition numbers $\kappa(\bar{M}_{\text{alt}}^{-1}\bar{K})$ of the ES-FEM and SSE method applied to the model linear elasticity problem (5.2) when n varies and n/N ($= H/h$) is fixed as 4.

In the NS-FEM, each element in \mathcal{T}_h is divided into three quadrilateral subdomains using its nodes, the midpoints of element edges, and the center point. The node-based smoothing domains consist of assemblages of adjacent subdomains belonging to different elements based on nodes; see Fig. 1(c). Denoting the collection of all smoothing domains constructed from \mathcal{T}_h for the NS-FEM by $\mathcal{S}_{h,\text{NS}}$, a smoothed gradient $\bar{\epsilon}^{(s)}$ for a smoothing domain $s \in \mathcal{S}_{h,\text{NS}}$ is defined by

$$\bar{\epsilon}^{(s)} = \frac{\sum_{k=1}^m |e^{(k)}| \epsilon^{(e^{(k)})}}{\sum_{k=1}^m |e^{(k)}|}, \quad (6.1)$$

where $e^{(k)}$ is the k th element in \mathcal{T}_h neighboring to the node corresponding to s , $\epsilon^{(e^{(k)})}$ was defined in (2.1), and m is the number of neighboring elements in \mathcal{T}_h . The number m varies node by node in general. Using the smoothed gradient in (6.1), the stiffness matrix \bar{K}_{NS} for the NS-FEM is defined in a similar manner as (2.5). It is known that the NS-FEM is effective in alleviating volumetric locking [3].

The following example shows that the NS-FEM in one-dimension is not spectrally equivalent to the standard FEM; examples corresponding to higher-dimensional cases can be constructed similarly.

Example 6.1. Let $\Omega = [0, 1] \subset \mathbb{R}$ and let \mathcal{T}_h be the uniform partition of Ω into n subintervals, where n is a positive even integer. In this case, the space V_h is defined as the collection of all piecewise linear and continuous functions on \mathcal{T}_h satisfying the homogeneous Dirichlet boundary condition. As depicted in Fig. 6(a), we set $u \in V_h$ such that

$$u\left(\frac{i}{n}\right) = \begin{cases} 0 & \text{if } i \text{ is even,} \\ 1 & \text{if } i \text{ is odd,} \end{cases} \quad i = 1, 2, \dots, n-1.$$

In each subinterval $i/n < x < (i+1)/n$, $i = 0, 1, \dots, n-1$, we have

$$u'(x) = \begin{cases} n & \text{if } i \text{ is even,} \\ -n & \text{if } i \text{ is odd.} \end{cases}$$

Applying the node-based smoothing to u' , we obtain the smoothed derivative \bar{u}'_{NS} as follows:

$$\bar{u}'_{\text{NS}}(x) = \begin{cases} n & \text{if } 0 < x < \frac{1}{2n}, \\ 0 & \text{if } \frac{1}{2n} < x < 1 - \frac{1}{2n}, \\ -n & \text{if } 1 - \frac{1}{2n} < x < 1. \end{cases}$$

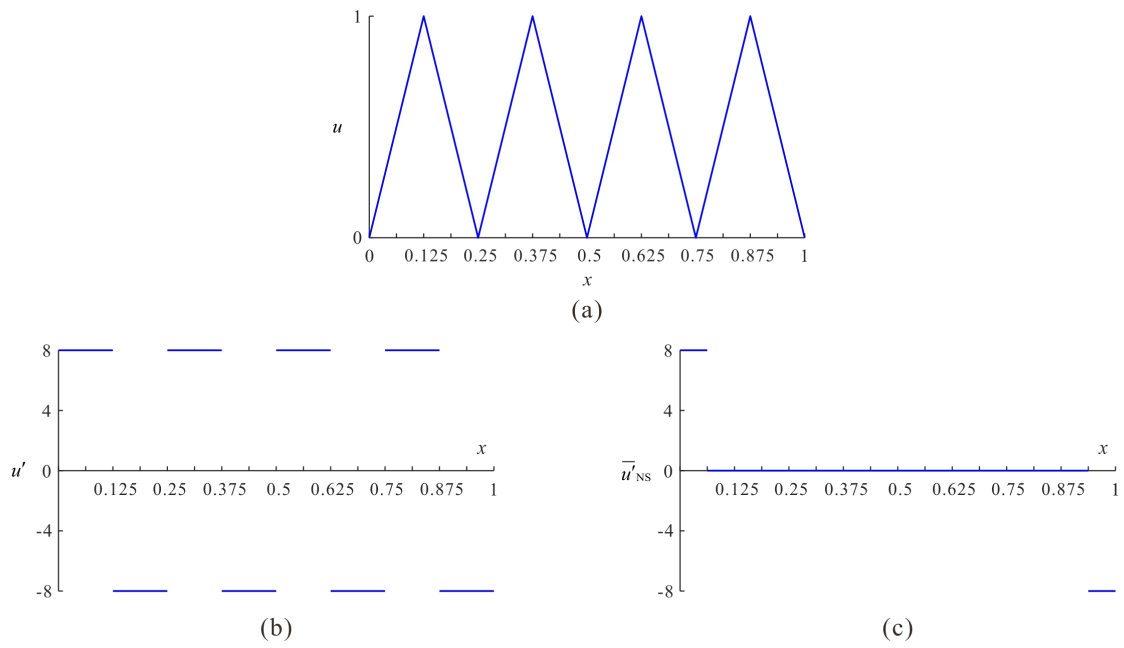


Figure 6: Graphs of (a) the function u , (b) its derivative u' , and (c) the node-based smoothed derivative \bar{u}'_{NS} in Example 6.1, when $n = 8$.

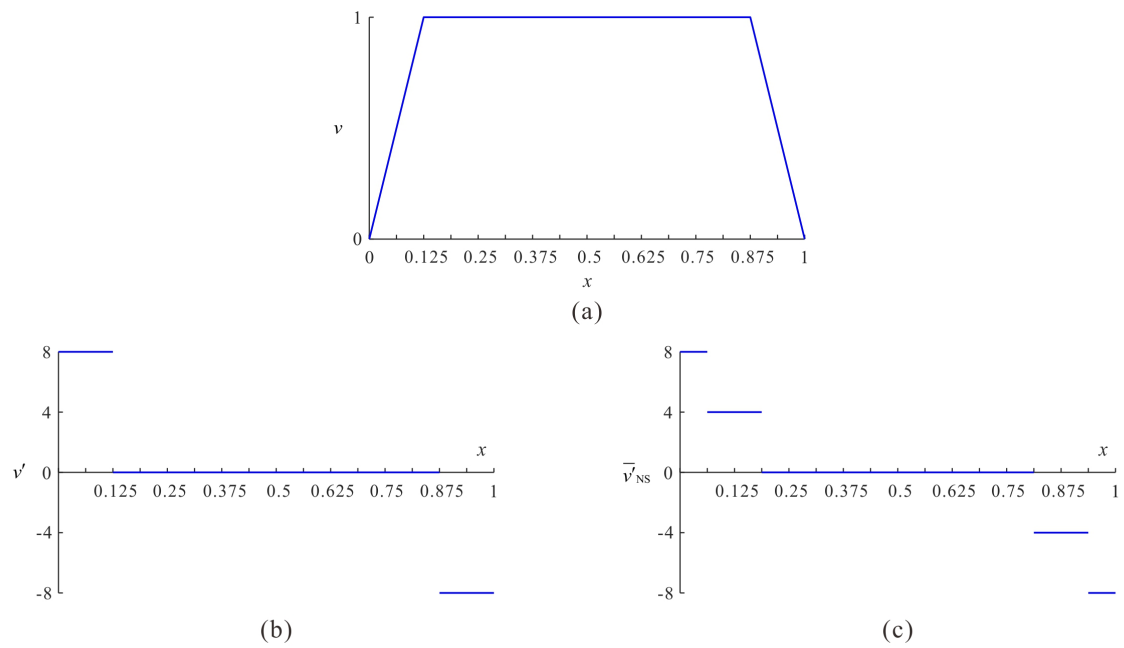


Figure 7: Graphs of (a) the function v , (b) its derivative v' , and (c) the node-based smoothed derivative \bar{v}'_{NS} in Example 6.1, when $n = 8$.

	$n = 2^3$	$n = 2^4$	$n = 2^5$	$n = 2^6$	$n = 2^7$
NS-FEM	9.36e1	3.75e2	1.53e3	6.21e3	2.50e4

Table 7: Condition numbers $\kappa(K^{-1}\bar{K}_{\text{NS}})$ for the model linear elasticity problem (5.2).

The graphs of u' and \bar{u}'_{NS} are plotted in Figs. 6(b) and (c), respectively. Hence, it follows that

$$\lambda_{\min}(K^{-1}\bar{K}_{\text{NS}}) \leq \frac{u^T \bar{K}_{\text{NS}} u}{u^T K u} = \frac{\int_{\Omega} |\bar{u}'_{\text{NS}}|^2 dx}{\int_{\Omega} |u'|^2 dx} = \frac{1}{n}. \quad (6.2)$$

Meanwhile, as shown in Fig. 7(a), we set $v \in V_h$ such that

$$v\left(\frac{i}{n}\right) = 1, \quad i = 1, 2, \dots, n-1.$$

Then one can readily obtain

$$v'(x) = \begin{cases} n & \text{if } 0 < x < \frac{1}{n}, \\ 0 & \text{if } \frac{1}{n} < x < 1 - \frac{1}{n}, \\ -n & \text{if } 1 - \frac{1}{n} < x < 1, \end{cases}$$

and

$$\bar{v}'_{\text{NS}}(x) = \begin{cases} n & \text{if } 0 < x < \frac{1}{2n}, \\ \frac{n}{2} & \text{if } \frac{1}{2n} < x < \frac{3}{2n}, \\ 0 & \text{if } \frac{3}{2n} < x < 1 - \frac{3}{2n}, \\ -\frac{n}{2} & \text{if } 1 - \frac{3}{2n} < x < 1 - \frac{1}{2n}, \\ -n & \text{if } 1 - \frac{1}{2n} < x < 1. \end{cases}$$

See Figs. 7(b) and (c) for the graphs of v' and \bar{v}'_{NS} , respectively. By direct calculation, we have

$$\lambda_{\max}(K^{-1}\bar{K}_{\text{NS}}) \geq \frac{v^T \bar{K}_{\text{NS}} v}{v^T K v} = \frac{\int_{\Omega} |\bar{v}'_{\text{NS}}|^2 dx}{\int_{\Omega} |v'|^2 dx} = \frac{3}{4}. \quad (6.3)$$

Combining (6.2) and (6.3) yields

$$\kappa(K^{-1}\bar{K}_{\text{NS}}) = \frac{\lambda_{\max}(K^{-1}\bar{K}_{\text{NS}})}{\lambda_{\min}(K^{-1}\bar{K}_{\text{NS}})} \geq \frac{3n}{4} = O(h^{-1}),$$

which implies that \bar{K}_{NS} and K are not spectrally equivalent.

We revisit the linear elasticity problem in Section 5.2; Table 7 provides the condition numbers $\kappa(K^{-1}\bar{K}_{\text{NS}})$ for various values of n . The result clearly shows that the stiffness matrix of the NS-FEM is not spectrally equivalent to that of the standard FEM; $\kappa(K^{-1}\bar{K}_{\text{NS}})$ increases approximately four times whenever n doubles. Table 8 presents the condition numbers of the M^{-1} -, \bar{M}^{-1} -, and $\bar{M}_{\text{alt}}^{-1}$ -preconditioned stiffness matrices and the corresponding conjugate gradient iteration counts #iter for the NS-FEM. As expected, the number of iterations and the condition number increase when n and N grow keeping the ratio n/N constant for all the preconditioners considered. In addition, it is numerically confirmed that the preconditioners \bar{M}^{-1} and $\bar{M}_{\text{alt}}^{-1}$ reduce the condition number to some extent, whereas the preconditioner M^{-1} does not.

7. Conclusion

Based on the fact that the stiffness matrices of the standard FEM, ES-FEM, and SSE method are spectrally equivalent, we proved that any existing preconditioners for the standard FEM can be applied to the ES-FEM and SSE method,

Precond.	N	$n = 2^3$		$n = 2^4$		$n = 2^5$		$n = 2^6$		$n = 2^7$	
		#iter	κ	#iter	κ	#iter	κ	#iter	κ	#iter	κ
None		60	4.03e2	112	1.40e3	204	5.19e3	393	1.99e4	743	7.81e4
M^{-1}	2	60	1.22e2	133	7.81e2	270	3.87e3	498	1.77e4	906	7.62e4
	2^2	-	-	116	4.47e2	269	3.26e3	515	1.58e4	943	6.54e4
	2^3	-	-	-	-	218	1.82e3	496	1.30e4	963	6.24e4
	2^4	-	-	-	-	-	-	389	7.25e3	906	5.14e4
	2^5	-	-	-	-	-	-	-	-	694	2.69e4
\bar{M}^{-1}	2	18	6.94e0	23	1.07e1	31	2.12e1	44	4.37e1	62	8.98e1
	2^2	-	-	29	1.80e1	37	3.70e1	54	8.23e1	78	1.76e2
	2^3	-	-	-	-	52	6.82e1	66	1.48e2	97	3.40e2
	2^4	-	-	-	-	-	-	95	2.74e2	119	6.03e2
	2^5	-	-	-	-	-	-	-	-	172	1.11e3
$\bar{M}_{\text{alt}}^{-1}$	2	18	7.85e0	24	1.10e1	32	2.16e1	45	4.39e1	63	8.99e1
	2^2	-	-	29	1.82e1	38	3.97e1	56	8.57e1	80	1.78e2
	2^3	-	-	-	-	52	6.93e1	69	1.62e2	102	3.59e2
	2^4	-	-	-	-	-	-	96	2.80e2	125	6.63e2
	2^5	-	-	-	-	-	-	-	-	173	1.13e3

Table 8: Condition numbers κ and iteration counts #iter of the NS-FEM applied to the model linear elasticity problem (5.2) with the two-level additive Schwarz preconditioners M^{-1} , \bar{M}^{-1} , and $\bar{M}_{\text{alt}}^{-1}$ defined in (4.1), (4.2), and (4.3), respectively.

inheriting good convergence properties such as numerical scalability. We also proposed the improved two-level additive Schwarz preconditioners for the ES-FEM and SSE method. It was shown both theoretically and numerically that the proposed preconditioners outperform the standard one when they are applied to the ES-FEM and SSE method.

This paper suggests several interesting topics for future research. Recall that the motivation for developing iterative solvers is a possibility of applying them to large-scale problems; we need to solve more complex engineering problems on a large scale using FEMs with strain smoothing equipped with the proposed preconditioners. Meanwhile, we observed in Section 6 that the spectral property of the NS-FEM is different from the ES-FEM and SSE method. This gives an evidence on that mathematical properties of the NS-FEM are somewhat different to those of other FEMs with strain smoothing. Hence, developing a mathematical theory on the NS-FEM should be considered as a separate work.

Appendix A. Convergence theory of additive Schwarz methods

In this appendix, we provide a brief summary on the abstract convergence theory of additive Schwarz methods introduced in [21, 29]. Let V be a Hilbert space. We consider the model linear problem

$$Au = f,$$

where $A: V \rightarrow V$ is a symmetric and positive definite linear operator and $f \in V$. In what follows, an index j runs from 1 to \mathcal{N} . For a Hilbert space V_j , we assume that there exists an interpolation operator $R_j^T: V_j \rightarrow V$ such that $V = \sum_{j=1}^{\mathcal{N}} R_j^T V_j$. Let $\tilde{A}_j: V_j \rightarrow V_j$ be a symmetric and positive definite linear operator which plays a role of a local operator on V_j . In this setting, the additive Schwarz preconditioner $M^{-1}: V \rightarrow V$ is given by

$$M^{-1} = \sum_{j=1}^{\mathcal{N}} R_j^T \tilde{A}_j^{-1} R_j.$$

In order to obtain an upper bound for the condition number of the preconditioned operator $M^{-1}A$, we need the following three assumptions.

Assumption Appendix A.1. There exists a constant $C_0 > 0$ which satisfies the following: for any $v \in V$, there exists $v_j \in V_j$, $1 \leq j \leq \mathcal{N}$, such that

$$v = \sum_{j=1}^{\mathcal{N}} R_j^T v_j$$

and

$$\sum_{j=1}^{\mathcal{N}} v_j^T \tilde{A}_j v_j \leq C_0^2 v^T A v.$$

Assumption Appendix A.2. There exists a constant $\tau_0 > 0$ which satisfies the following: for any $v_j \in V_j$, $1 \leq j \leq \mathcal{N}$, and $\tau \in (0, \tau_0]$, we have

$$\left(\sum_{j=1}^{\mathcal{N}} R_j^T v_j \right)^T A \left(\sum_{j=1}^{\mathcal{N}} R_j^T v_j \right) \leq \frac{1}{\tau} \sum_{j=1}^{\mathcal{N}} (R_j^T v_j)^T A (R_j^T v_j).$$

Assumption Appendix A.3. There exists a constant $\omega_0 > 0$ which satisfies the following: for any $v_j \in V_j$, $1 \leq j \leq \mathcal{N}$, we have

$$(R_j^T v_j)^T A (R_j^T v_j) \leq \omega_0 v_j^T \tilde{A}_j v_j.$$

For detailed explanations of the above assumptions, one may refer to [21, 29]. Under Assumptions Appendix A.1, Appendix A.2, and Appendix A.3, we define the additive Schwarz condition number κ_{ASM} as follows:

$$\kappa_{\text{ASM}} = \frac{\omega_0 C_0^2}{\tau_0}, \quad (\text{A.1})$$

where C_0 , τ_0 , and ω_0 are chosen as optimal as possible. That is, C_0 is chosen as the minimum one satisfying Assumption Appendix A.1, τ_0 as the maximum one satisfying Assumption Appendix A.2, and ω_0 as the minimum one satisfying Assumption Appendix A.3. The following theorem says that the convergence rate of a preconditioned iterative algorithm for $M^{-1}A$ relies on the additive Schwarz condition number κ_{ASM} [29].

Theorem Appendix A.4. *Under Assumptions Appendix A.1, Appendix A.2, and Appendix A.3, we have*

$$\frac{\tau_0}{\omega_0} v^T A v \leq v^T M v \leq C_0^2 v^T A v \quad \forall v \in V.$$

Consequently, the following holds:

$$\kappa(M^{-1}A) \leq \kappa_{\text{ASM}},$$

where κ_{ASM} was given in (A.1).

References

- [1] J. S. Chen, C. T. Wu, S. Yoon, Y. Y. A stabilized conforming nodal integration for Galerkin mesh-free methods, *International Journal for Numerical Methods in Engineering* 50 (2001) 435–466.
- [2] G. R. Liu, K. Y. Dai, T. T. Nguyen, A smoothed finite element method for mechanics problems, *Computational Mechanics* 39 (2007) 859–877.
- [3] G. R. Liu, T. Nguyen-Thoi, H. Nguyen-Xuan, K. Y. Lam, A node-based smoothed finite element method (NS-FEM) for upper bound solutions to solid mechanics problems, *Computers & Structures* 87 (2009) 14–26.
- [4] G. R. Liu, T. Nguyen-Thoi, K. Y. Lam, An edge-based smoothed finite element method (ES-FEM) for static, free and forced vibration analyses of solids, *Journal of Sound and Vibration* 320 (2009) 1100–1130.
- [5] G. R. Liu, T. Nguyen-Thoi, *Smoothed Finite Element Methods*, CRC Press, New York, 2010.
- [6] A. Hamrani, S. H. Habib, I. Belaidi, CS-IGA: A new cell-based smoothed isogeometric analysis for 2D computational mechanics problems, *Computer Methods in Applied Mechanics and Engineering* 315 (2017) 671–690.
- [7] W. H. Yuan, B. Wang, W. Zhang, Q. Jiang, X. T. Feng, Development of an explicit smoothed particle finite element method for geotechnical applications, *Computers and Geotechnics* 106 (2019) 42–51.
- [8] H. Nguyen-Xuan, S. Bordas, H. Nguyen-Dang, Smooth finite element methods: convergence, accuracy and properties, *International Journal for Numerical Methods in Engineering* 74 (2008) 175–208.
- [9] G. R. Liu, H. Nguyen-Xuan, T. Nguyen-Thoi, A theoretical study on the smoothed FEM (S-FEM) models: Properties, accuracy and convergence rates, *International Journal for Numerical Methods in Engineering* 84 (2010) 1222–1256.

- [10] C. Lee, P. S. Lee, A new strain smoothing method for triangular and tetrahedral finite elements, *Computer Methods in Applied Mechanics and Engineering* 341 (2018) 939–955.
- [11] C. Lee, P. S. Lee, The strain-smoothed MITC3+ shell finite element, *Computers & Structures* 223 (2019) 106096.
- [12] C. Lee, S. Kim, P. S. Lee, The strain-smoothed 4-node quadrilateral finite element, *Computer Methods in Applied Mechanics and Engineering* 373 (2021) 113481.
- [13] C. Lee, J. Park, A variational framework for the strain-smoothed element method, *Computers & Mathematics with Applications* 94 (2021) 76–93.
- [14] W. Zeng, G. Liu, Smoothed finite element methods (S-FEM): an overview and recent developments, *Archives of Computational Methods in Engineering* 25 (2018) 397–435.
- [15] C. Farhat, F.-X. Roux, Implicit parallel processing in structural mechanics, *Computational Mechanics Advances* 2 (1994) 1–124.
- [16] Y. Saad, *Iterative Methods for Sparse Linear Systems*, SIAM, Philadelphia, 2003.
- [17] B. F. Smith, An optimal domain decomposition preconditioner for the finite element solution of linear elasticity problems, *SIAM Journal on Scientific and Statistical Computing* 13 (1992) 364–378.
- [18] A. Klawonn, L. F. Pavarino, Overlapping Schwarz methods for mixed linear elasticity and Stokes problems, *Computer Methods in Applied Mechanics and Engineering* 165 (1998) 233–245.
- [19] M. Griebel, D. Oeltz, M. A. Schweitzer, An algebraic multigrid method for linear elasticity, *SIAM Journal on Scientific Computing* 25 (2003) 385–407.
- [20] C. R. Dohrmann, O. B. Widlund, An overlapping Schwarz algorithm for almost incompressible elasticity, *SIAM Journal on Numerical Analysis* 47 (2009) 2897–2923.
- [21] A. Toselli, O. Widlund, *Domain Decomposition Methods—Algorithms and Theory*, Springer, Berlin, 2005.
- [22] L. B. Da Veiga, D. Cho, L. Pavarino, S. Scacchi, Isogeometric Schwarz preconditioners for linear elasticity systems, *Computer Methods in Applied Mechanics and Engineering* 253 (2013) 439–454.
- [23] J. G. Calvo, An overlapping Schwarz method for virtual element discretizations in two dimensions, *Computers & Mathematics with Applications* 77 (2019) 1163–1177.
- [24] D. Cho, L. Pavarino, S. Scacchi, Overlapping additive Schwarz preconditioners for isogeometric collocation discretizations of linear elasticity, *Computers & Mathematics with Applications* 93 (2021) 66–77.
- [25] J. Xu, Iterative methods by space decomposition and subspace correction, *SIAM Review* 34 (1992) 581–613.
- [26] J. Xu, The method of subspace corrections, *Journal of Computational and Applied Mathematics* 128 (2001) 335–362.
- [27] T. Nguyen-Thoi, G. R. Liu, H. Nguyen-Xuan, An n-sided polygonal edge-based smoothed finite element method (nES-FEM) for solid mechanics, *International Journal for Numerical Methods in Biomedical Engineering* 27 (2011) 1446–1472.
- [28] G. R. Liu, A G space theory and a weakened weak (W2) form for a unified formulation of compatible and incompatible methods: Part I theory, *International Journal for Numerical Methods in Engineering* 81 (2010) 1093–1126.
- [29] J. Park, Additive Schwarz methods for convex optimization as gradient methods, *SIAM Journal on Numerical Analysis* 58 (2020) 1495–1530.